Mosquito Larval Habitat Mapping Using Remote Sensing and GIS: Implications of Coalbed Methane Development and West Nile Virus

LI ZOU,[1] SCOTT N. MILLER,[1] AND EDWARD T. SCHMIDTMANN[2]

J. Med. Entomol. 43(5): 1034–1041 (2006)

ABSTRACT Potential larval habitats of the mosquito *Culex tarsalis* (Coquillett), implicated as a primary vector of West Nile virus in Wyoming, were identified using integrated remote sensing and geographic information system (GIS) analyses. The study area is in the Powder River Basin of north central Wyoming, an area that has been undergoing a significant increase in coalbed methane gas extractions since the late 1990s. Large volumes of water are discharged, impounded, and released during the extraction of methane gas, creating aquatic habitats that have the potential to support immature mosquito development. Landsat TM and ETM+ data were initially classified into spectrally distinct water and vegetation classes, which were in turn used to identify suitable larval habitat sites. This initial habitat classification was refined using knowledge-based GIS techniques requiring spatial data layers for topography, streams, and soils to reduce the potential for overestimation of habitat. Accuracy assessment was carried out using field data and high-resolution aerial photography commensurate with one of the Landsat images. The classifier can identify likely habitat for ponds larger than 0.8 ha (2 acres) with generally satisfactory results (72.1%) with a lower detection limit of ≈0.4 ha (1 acre). Results show a 75% increase in potential larval habitats from 1999 to 2004 in the study area, primarily because of the large increase in small coalbed methane water discharge ponds. These results may facilitate mosquito abatement programs in the Powder River Basin with the potential for application throughout the state and region.

KEY WORDS *Culex tarsalis*, risk, discharge water

Accurate mapping of the spatial distribution of mosquito breeding habitats is essential for cost-effective deployment of control practices. Geospatial mapping by using remote sensing offers the potential to identify larval habitats on a large area basis to a degree that is difficult or impossible using conventional ground survey (Hayes et al. 1985, Washino and Wood 1994, Dale et al. 1998, Hay et al. 1998). The objective of this study is to assess potential larval habitats of *Culex tarsalis* (Coquillett) by using Landsat TM imagery in the Powder River Basin of northern Wyoming in an effort to establish a basis for predicting risk of exposure to West Nile virus. Mosquitoes of the genus *Culex* are the dominant disease vector and transmitter of the West Nile Virus (Hayes 1989, Goddard et al. 2002). In Wyoming, the primary vector species is *Culex tarsalis* (E.T.S., unpublished data).

Mosquito control is a critical component of the arbovirus control programs, and one of the most effective ways to control a mosquito population is to reduce its larval (breeding) habitats. Previous studies have shown benefits of using remote sensing in the identification of mosquito breeding habitats (Linthicum et al. 1987, Pope et al. 1992, Wood et al. 1992, Dale and Morris 1996, Thomson et al. 1996, Masuoka et al. 2003). However, these studies have not targeted West Nile Virus or the intermountain West and plains areas in Wyoming where West Nile Virus risk is high. Rogers et al. (2002) used AVHRR 1-km resolution data set to create a West Nile virus risk map in North America. From an operational point of view, the map resolution is too coarse to implement local control strategies and is not specific to larval habitat. With the increasing status of this emerging arbovirus, a more accurate and finer grained mapping system is necessary to aid the West Nile Virus prevention program. Landsat TM data has proven to be an excellent choice for environmental studies in past 26 yr. Landsat spectral data, particularly band 4 (infrared) and band 5 (mid-infrared) are well suited for vegetation and water content analysis, and data are collected at a scale suitable for regional and local analysis. For these reasons Landsat TM data were chosen as the base imagery for larval habitat assessment.

Since West Nile Virus arrived in New York City in 1999, it has spread across the North American continent (Enserink 2002), and by the end of 2004, the total human deaths reached 374 cases nationwide. The state of Wyoming was hit heavily in 2003 with 375 human cases, including nine deaths (CDC 2004). In addition to posing a clear threat to human health, the West Nile

[1] Department of Renewable Resources, University of Wyoming, Box 3354, 1000 E. University Ave., Laramie, WY 82071.
[2] Arthropod-Borne Animal Disease Research Laboratory, USDA–ARS, Box 3965, University Station, Laramie, WY 82070.

0022-2585/06/1034–1041$04.00/0 © 2006 Entomological Society of America

Virus poses a threat to native wildlife species. For example, the West Nile Virus is hypothesized to be responsible for the sharp decline of greater sage-grouse, *Centrocercus urophasianus*, in this region because the survival rate of this species has been reduced by 25% in recent years (Naugle et al. 2004). Of importance to potential management and control strategies in this area, the greater sage-grouse is an ecologically threatened species in the United States, and there is concern regarding the impact of the virus on sage grouse populations throughout the West (Naugle et al. 2004). At a minimum, alterations to the landscape and subsequent threats to wildlife and people indicate that monitoring and controlling the West Nile virus is a critical and potentially long-term commitment (Morse 2003) requiring a temporal and spatial strategy.

In general, *Cx. tarsalis* are small standing water species. Gravid females are attracted to water with high organic matter (Beehler and Mulla 1995) and larvae of *Cx. tarsalis* feed on organic debris in water that has a very little disturbance either in the form of wave action or flow. In a natural environment, larval habitats of *Cx. tarsalis* are often associated with vegetation growing at pond edges (Reisen 1993). More specifically, the edges of small water bodies where vegetation and other debris are concentrated are identified as larval microhabitat. Large water bodies (usually larger than 4 ha [10 acres]) that are exposed to wind and wave action, and running water such as a river or stream, are not suitable for larval development. Open waters are also unsuitable because larvae and pupae are vulnerable to predation (Laird 1988). Nutrition concentrations in open water region and running streams are generally much lower than pond edges and small standing water (Laird 1988). According to a survey conducted by Denke and Spackman (1990), the majority of mosquito-breeding habitats in Wyoming are created by human activities. In the Powder River Basin, human-made water storages, such as livestock watering ponds and discharge water ponds used in coalbed methane (CBM) development (natural gas) constitute the most likely breeding and larval habitats for *Cx. tarsalis* (Fig. 1).

CBM is a naturally occurring gas contained within unexposed coal beds. Recently strong demand makes it potentially highly profitable to extract CBM from buried coal seams. Water is a critical component in this system, because gas is held in place by water pressure. To extract methane, the water must be removed to allow the gas to flow freely from the coal, in a process referred to as "dewatering" (Nuccio 2001). The amount of water produced in this manner is considerable. Rice et al. (2000) estimated that >1.28 million barrels of water was produced each day from CBM extraction in 2000. Wyoming has witnessed a sharp increase in CBM discharge ponds associated with the development of CBM fields throughout the state, particularly the Powder River Basin in northern Wyoming because it has experienced the greatest growth in volume of discharge water and numbers of wells and ponds over the past decade (WOGCC 2005). Vast quantities of methane gas occur in association with shallow coal beds (24,000 feet in depth) that underlie the Powder River Basin in north central Wyoming. Since 1999 when it became economically feasible to tap natural gas in the Powder River Basin, ≈19,000 CBM wells have been drilled, and ≈20,000 additional wells are projected over the next decade. Total recoverable production of coproduced water in the Powder River Basin alone exceeds 5.5 million acre-feet (DOE 2002). In the study area, the majority of coproduced water is discharged onto the surface and into small detention basins, leading to an increase in small water bodies. These recent increases in ponded water are hypothesized to increase WNV risk because CBM ponds may serve as suitable habitat for larval *Cx. tarsalis.*

Materials and Methods

Data and Software. The basic research strategy was to 1) develop habitat classification techniques using historical imagery, 2) classify two images using these techniques to capture the temporal and spatial changes in habitat, 3) validate these techniques by using a combination of field observations and high resolution aerial photography.

Landsat TM images and other GIS data were obtained from the WyomingView data repository via the Wyoming Geographic Information Center download site (http://www.wygisc.uwyo.edu/clearinghouse). Three images were selected for use in this study that capture the temporal and spatial changes: 12 August 2004 (Landsat 5 TM), 14 August 2001 (Landsat 7 ETM+), and 9 August 1999 (Landsat 7 ETM+). The ETM+ images are USGS L1-T products that have been processed for radiometric, geometric, and terrain corrections. The 1999 and 2004 images serve as end members for change detection, whereas the 2001 image was classified as a separate validation data set and compared against high-resolution photography taken at approximately the same time. The TM image has been corrected for radiometric and geometric distortions. Spatial data used in the GIS portion of this research were National Elevation Dataset for Wyoming (DEM; 30-m spatial resolution), National Land Cover Dataset for Wyoming (NLCD; 30-m spatial resolution), and major hydrography features. Color infrared Digital Orthophoto Quarter Quads (DOQQs; 1-m spatial resolution acquired in July 2001) were downloaded from the Wyoming Spatial Data Clearinghouse (http://wgiac2.state.wy.us) for validation of the 2001 imagery.

An integrated raster (image classification) and vector (GIS) analysis was used to refine the identification of *Cx. tarsalis* larval habitat. Image classification was conducted using the ERDAS IMAGINE 8.7 (Leica Geosystems GIS & Mapping, LLC, Atlanta, GA). Image processing algorithms in this paper are cited at ERDAS documentation (ERDAS, Inc. 2003).

To address that suitable habitat may be defined as the junction between riparian vegetation and water, a GIS-based spatial analysis procedure was implemented in ArcGIS 9.0 (ESRI, Redlands, CA) to union

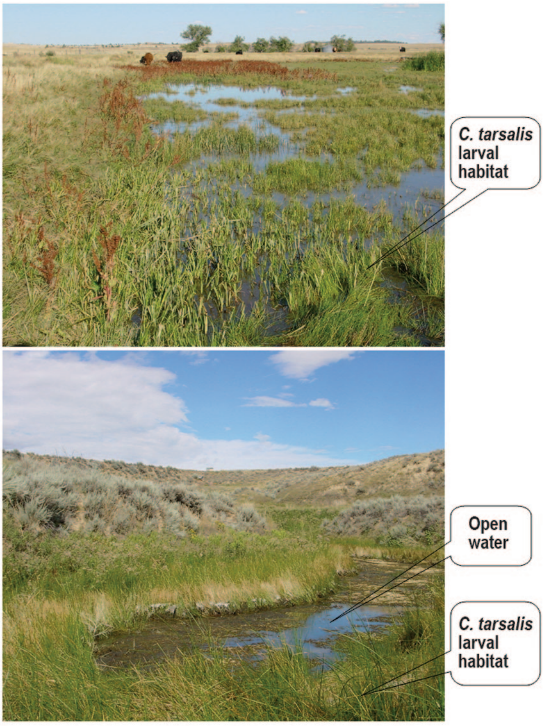

Fig. 1. Discharge pools of CBM development. The *Cx. tarsalis* larval habitat is the vegetation at the pond edges.

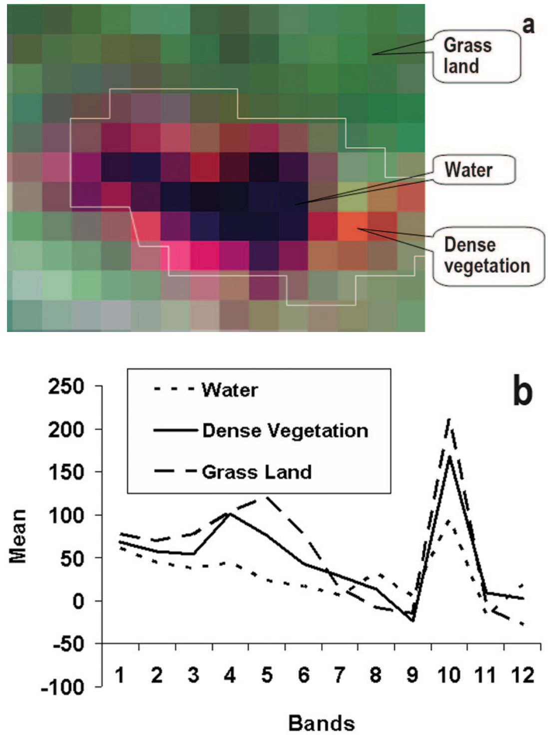

Fig. 2. (A) Typical larval habitat of *Cx. tarsalis* in the Landsat TM image (red, band 4; green, band 5; blue, band 3). The circled area is the Areas of interest. (B) Bands in spectral reflectance graph are as follows: Landsat TM, bands 1–6; NDVI*100, band 7; NDWI*100, band 8; flood index*100, band 9; Tasseled cap transformation bands 10, brightness; 11, greenness; and 12, wetness.

all dense vegetations identified from panchromatic band and any riparian vegetation located at the edges of water bodies. Union is a process of merging overlapping multiple features into a single feature. All such pixels were classified as potentially suitable habitats. Selected habitats were exported into an ArcGIS format shapefile for refinement by using GIS techniques.

Based on the factor that large water bodies and flowing streams are not suitable for larval development of *Cx. tarsalis*, pixels that spatially intersected or abutted these features were eliminated. Large open water bodies larger than 4 ha were identified using standard patch analysis. Small digitization and georectification errors may cause discontinuities between the imagery and GIS data sets, resulting in the outcome that stream lines do not always directly overlap with corresponding water and riparian classes in classified images. A 30-m buffer zone was created to ensure that pixels of major streams in the classified images intersected with their GIS-based vector counterparts. Potential habitat that intersected with the buffered major stream vector data were excluded from the final classified map.

Another potential source of error occurs where shadows from hillside or forest areas are misclassified as water; these areas were eliminated by only allowing classified habitat pixels to be present on slopes $<5°$. This approach served the dual purpose of removing areas where water is flowing due to gravity from consideration under the premise that larval habitat is dependent on stagnant or very slow-moving water.

Image Classification. From a false color composite Landsat TM image, a typical larval habitat of *Cx. tarsalis* can be recognized as a mosaic of several dark pixels (water) adjacent to red pixels (vegetation) (Fig. 2). Areas of interest (AOI) were delineated by selecting pixels in known larval-positive sites (Fig. 2). Because of limited access to the area due to private landholdings, field samples could not cover all combinations of land cover types identified in the scene. To compensate for uneven access to the study area and to create a more evenly distributed set of training data, additional areas of interest were manually selected according to field experiences and familiarity with the region. In addition to six bands of Landsat TM data, several variables that may contribute to the image classification were derived and stacked with original images. These variables are: Normalized difference vegetation index (NDVI); flooding index (FI; Philipson and Hafker 1981); Normalized Difference Water Index (NDWI; Gao 1996), and Tasseled cap transformation (Kauth and Thomas 1976, Crist and Cicone 1984).

The classification workflow is shown as Fig. 3. An unsupervised classification (Iterative Self-Organizing Data Analysis Technique; ISODATA) was used to generate four classes in the areas of interest extracted

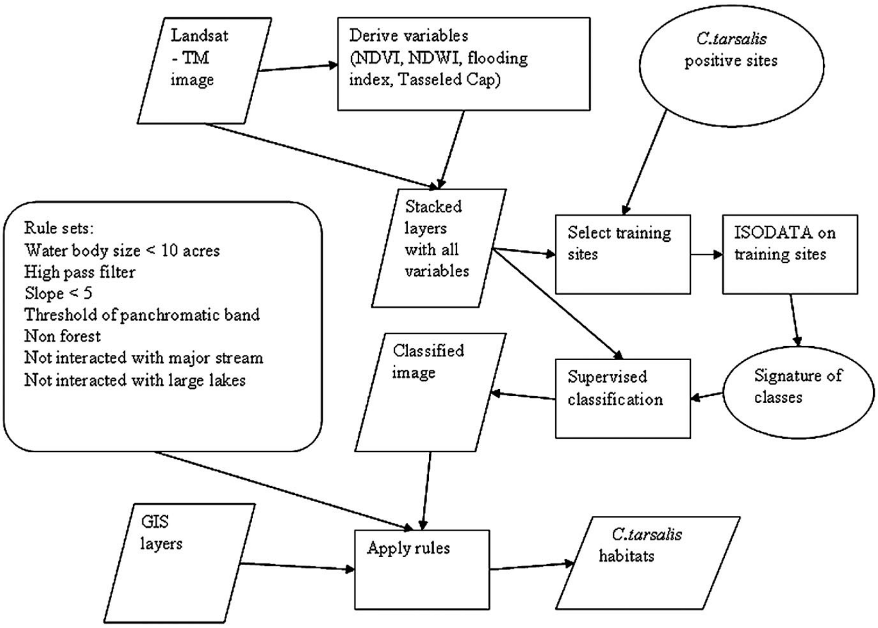

Fig. 3. Workflow of classification of *Cx. tarsalis* larval habitats.

from the positive sites from field sampling. The mean of each cluster is determined by an iterative process to meet the condition that each pixel is assigned to the class with the minimum distance (see equation). Iterations stop when the convergence threshold T, normalized percentage of pixels without change of assignment, is reached (in this case, T reached the threshold of 95% at iteration 3). A fifth class was added into the signature editor by using grassland pixels extracted from an AOI because grasslands are the dominant background vegetation type surrounding water and emergent vegetation. Using the signature generated from ISODATA, a supervised classification was conducted to classify the image. The parameter setting is as follows: nonparametric rule (parallelpiped), overlap rule (parametric rule), unclassified rule (parametric rule), and parametric rule (minimum distance). First, a candidate pixel is subjected to parallelpiped classification in which a pixel is assigned within the limits of mean ± SD of each class. Second, pixels in the overlapping region of classes or left without assignment to any class in parallelpiped classification are assigned to the closest class by using the parametric rule of minimum distance (see equation). The spectral distance from pixel *x*, *y* to the mean of class c is defined as SD_{xyc} by using the equation:

$$SD_{xyc} = \sqrt{\sum_{i=1}^{n} (\mu_{ci} - X_{xyi})^2}$$

where X_{xyi} is data file value of pixel *x*, *y* in band *i*, and μ_{ci} is mean of data file values in band *i* for the sample for class *c*.

These five classified classes were compressed into three classes: water, dense vegetations, and grasslands and shrubs. *Cx. tarsalis* larval habitat was represented as dense vegetation immediately adjacent to small water bodies. The habitats were extracted from classified images to meet these criteria. Final habitats were generated using rule based modeling according to the knowledge from experts and our field experiences.

Accuracy Assessment. A field study was undertaken in August 2004 to identify *Cx. tarsalis* larval habitats. Sampling coordinates were recorded using a geographic positioning system and transformed into a GIS data layer. Mosquito larvae were collected along pond edges by using a standard dipper. For each site, four dipping were taken every 5 m with a total distance of 100 m. Collected larvae were sorted by species at the USDA–ARS Arthropod Borne Animal Disease Research Laboratory in Laramie, WY. Sites were classified as positive if larvae of *Cx. tarsalis* were identified. Sites positive for *Cx. tarsalis* were overlaid with the image and used as training sites for the extraction of appropriate spectral signatures.

The classified result from the 14 August 2001 image was compared against the DOQQs on 1 July 2001 for an accuracy assessment. The area covered by the DOQQs is ≈171,450 ha. All small water bodies (excluding running rivers) in the DOQQs were digitized by hand as a proxy for ground truth. As noted, this area is highly dynamic due to the very rapid pace of CBM development, and the use of aerial photography serves as a static data layer that was coincident in timing with the satellite overpass. Ponds with area larger than ≈0.04 ha (≈0.1 acre) were used as the reference (equivalent to 1 pixel size in Landsat TM images, 30 by 30 m). The error matrix was computed using the final classified results and digitized ponds.

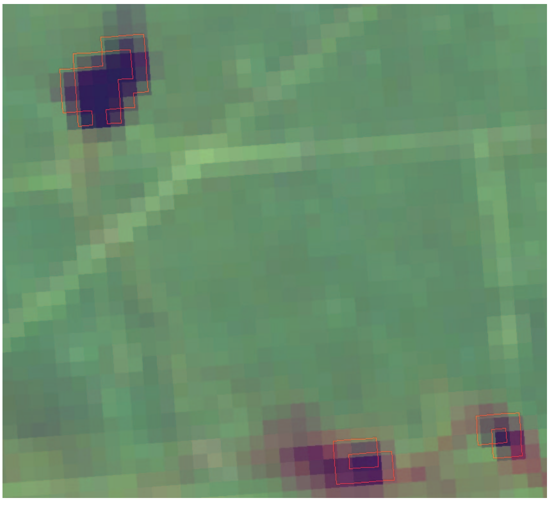

Fig. 4. Section of classified map of *Cx. tarsalis* larval habitats. The habitats are shown as the ring-shaped polygons covering the area of vegetation adjacent to small water bodies.

Results

Spectral Analysis and Interpretation of Classes. The spectral reflectance curves of classified classes generated from the ISODATA are illustrated in Fig. 2. From the spectrum of the original five classes and the comparison of raw imagery and the aerial photo, these classes were compressed into three distinct classes: water, dense vegetations, and grasslands and shrubs. Dense vegetations in the study area are predominantly herbaceous materials associated with high soil moisture that consequently has higher values in the NDWI (band 8) and the wetness index (band 12). Grasslands and shrubs occupy portions of the image that are more typically open and dry landscapes where the soil moisture content is lower. Their presence is indicated by higher brightness value (band 10) and lower values in the NDWI (band 8) and the wetness index (band 12).

Based on field observations, we consider that the primary larval habitats of *Cx. tarsalis* are where riparian vegetation is immediately adjacent to small water bodies. In our classification system riparian vegetation falls under the general classification of "dense vegetation," and habitat is identified in locating small water bodies and performing a proximal analysis to dense vegetation that represents emergent and riparian communities. Grasslands and shrubs are not considered as indicators or suitable larval habitats. A high pass 30-m filter was created to identify dense vegetation class immediately adjacent to water class, and these pixels were identified as *Cx. tarsalis* larval habitats.

Refinement of Classified Image for Habitat Suitability by Using Spatial Analysis. A scale issue was identified in the classification and field identification process: some very small ponds, usually smaller than 2 to 3 pixels, were improperly not classified as open water because they are mixed pixels in Landsat TM images. A significant number of these mixed pixels were classified as dense vegetations and are more properly classified as potential *Cx. tarsalis* larval habitats. Indeed, small standing water bodies have a greater potential for larval development than large open bodies of water, so identifying and classifying small bodies with adjacent dense vegetation is important but challenging given the limitation of pixel resolution. To refine these "missing" habitats, a secondary classification was performed by setting a threshold of exceedance in the panchromatic band, which has a higher spatial resolution (15 m). A rule set was established to filter out all dense vegetation pixels with a patch size smaller than 5 pixels (multispectral bands) because these small patches have the potential to be mixed water/riparian pixels in the 30-m data. These candidate pixels were further screened by eliminating the area where the digitial number (DN) value in the panchromatic was above a threshold set individually for each image (DN = 43 for 2001). Small patches with panchromatic DN less than the threshold are therefore classified as suitable habitat.

This refinement was performed for the 2001 image only. The 2004 image is Landsat 5 (Landsat 7 data are unavailable because of satellite equipment malfunction), which does not have a panchromatic band. These satellites are suitable for comparative analysis because they have exactly the same spectral range in bands 1–6. Although the habitat class in 2001 image accounts for ≈15.7% of all suitable habitats, there does not seem to be a temporal trend in the type and size of CBM discharge ponds in the study area. By losing access to the panchromatic band and not identifying habitat classes, we are underpredicting potential *Cx. tarsalis* habitat but not biasing the results with differential methods for the imagery. Future research will focus on higher spatial and spectral resolution data sets

Table 1. Error matrix of classification of *Cx. tarsalis* larval habitat

Classified image	Color infrared photo					Total	CA %
	>4 acres	>3 acres	>2 acres	>1 acre	>0.22 acre		
Habitat	14	18	49	99	185	211	87.68
Nonhabitat	2	6	19	62	257		
Total	16	24	68	161	442		
PA %	87.5	75.0	72.06	61.49	41.86		

CA, consumer's accuracy; PA, producer's accuracy. An area of 0.22 acre is equal to 1 pixel size in Landat TM images (30 by 30 m) (1 acre = 4,046.86 m^2).

Table 2. Classes resulting from unsupervised/supervised classification of the Powder River Basin

Feature	1999 ha	2004 ha	% increase
Water	478.8	836.9	74.8
Habitats	619.0	1084.5	75.2

1 ha = 10,000 m^2.

to isolate and identify small patches of potential larval habitat.

The final product generated from the classification procedure is shown as Fig. 4. By comparing the classified results with digitized small ponds in DOQQs, an error matrix was calculated and is presented as Table 1. Ponds are divided into different categories by their sizes because pond size is a primary limiting factor in the classification. Ponds smaller than the size of 1 pixel were not considered in this study, and we think that attempting to identify these ponds is beyond the capability of the Landsat TM images. The producer's accuracy reflects how well a pond on the ground (reality) is properly identified, and it is satisfactory for ponds larger than 0.8 ha (2 acres) (>70%). The producer's accuracy drops down to 61.5% after the pond size is smaller than 0.4 ha (1 acre). Overall, the consumer's accuracy, defined as how correct classified pond feature are, is ≈88%, indicating that the risk of overestimating habitat, primarily by inappropriately identifying vegetation not associated with small water bodies, is acceptable from a management perspective.

There was a 75.2% increase on the areas of potential larval habitats of *Cx. tarsalis* from 1999 to 2004 (Table 2; Fig. 5). This increase corresponds strongly to a commensurate 74.8% increase in area covered by water. Total area that falls into habitat increased from ≈619 to ≈1,100 ha. This correlation indicates the relative efficiency in the establishment of mosquito habitat with the increase in surface water. Given that CBM development is the primary source of new standing water bodies in this region, the observed increase in aquatic habitat with the potential to support larval mosquito populations is directly linked to growth in the CBM production.

Discussion

This study provides a method to rapidly assess potential larval habitats of *Cx. tarsalis* at a large spatial scale in a cost-effective way. The spatial proximity and size of water and dense vegetations are critical to separate larval habitats of *Cx. tarsalis* from other water and vegetation features. The classification procedure presented here successfully models potential larval habitats for water bodies larger than 0.8 ha (2 acres). The advantage of explicitly defining the spectral range and spatial relationship among habitat elements is that the ecological niche of larval habitat can be more precisely separated from other features. Results from the accuracy assessment indicate that the classification accuracy depends on the relative percentages of different sizes of water bodies. However, due to the spatial resolution of Landsat TM images (2–3 pixels), the classification will underestimate possible larval habitats in regions where the majority of water bodies are less than 0.8 ha (2 acres). The spectral signatures of these small areas are not separable from the signatures of other features such as streams and shadows of hillsides.

The average annual increase in CBM production from the Powder River Basin has been 66% since the mid-1990s, with a more rapid rate of growth after 2000 (Wyoming Outdoor Council and Powder River Basin Resource Council 2004). CBM development over the study period was extracted from online data published by WOGCC (2005). Wells have produced water were 1,784 in 1999, 8,941 in 2001 and 16,572 in 2004. The link between individual well production and location or concentration of surface discharge is lacking; wells are generally linked via a manifold and pond or surface discharges are not dependent on the location or number of wells. As such, the number of productive wells is a proxy for growth and potential releases of water. This relationship underscores the need for active assessment, because the spatial distribution of ponds and water releases is not predictive of the potential for larval habitat growth and cannot be used as a management tool.

According to the U.S. Geological Survey (2004), the Powder River Basin accounts for 30% in 2002 and 70% in 2003 of all human cases of the West Nile virus in Wyoming. Data from image classification presented here documented the dramatic increase of water discharge pools that are potential larval development sites for *Cx. tarsalis.* The methodology used in these analyses and results from changing land cover analyses can assist local authorities in the prioritization of sites for West Nile virus prevention programs. In addition,

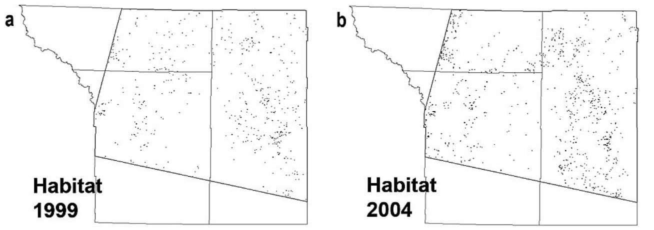

Fig. 5. Classified larval habitats of *C. tarsalis* in 1999 and 2004 inside Landsat TM cover area (Sheridan, Johnson, and Campbell counties).

the modeled larval habitats can be integrated into a global positioning system-guided control operation.

Although the risk of West Nile virus is determined by many factors, such as temperature and avian host availability, *Cx. tarsalis* habitats as a source of contribution continues to increase because of the thriving CBM development in this region. *Cx. tarsalis* larval habitat is associated with ponds that are water sources for many wildlife species and domestic animals such as cattle. These animals are in very close contact with infected *Cx. tarsalis.* Naugle et al. (2004) showed the decline of greater sage-grouse in this region in recent years with correlations to increased CBM activities.

The classification procedure developed in this study can be used to efficiently create a spatially explicit distribution of *Cx. tarsalis* larval habitats at the large scale. Although ponds smaller than one acre will be overlooked in this assessment, the product is valuable for the regional prediction of the vector population. Estimates of larval habitat are a conservative estimate but reflect the underlying spatial variability and density of risk. Given that permanent water stands are usually larger than 0.8 ha (2 acres), results from this study are suitable for long-term monitoring purposes. We are currently pursuing the use of higher spatial resolution images, to improve the resolution of spatial assessment and to better quantify the impact of CBM discharge water on mosquito larval habitat for ponds smaller than the detectable limit with Landsat.

Because *Culex* spp. mosquitoes are primary vectors of West Nile virus, the methods and activities in this study may provide a tool to identify *Culex* species habitats in other regions of North America. The image classification can be easily repeated and adopted. With the wide availability of Landsat TM data, this classification procedure can be applied more broadly in the future.

Acknowledgments

We thank Colleen Boodleman for work digitizing ponds from the DOQQs. This manuscript was improved by comments from Ramesh Sivanpillai. This work was supported by grants from USDA–ARS. The manuscript was approved for publication by the director of USDA–ARS.

References Cited

Beehler, J. W., and M. S. Mulla. 1995. Effects of organic enrichment on temporal distribution and abundance of culicine egg rafts. J. Am. Mosq. Control Assoc. 11: 167–171.

[CDC] **Centers for Disease Control and Prevention. 2004.** West Nile Virus Activity—United States, November 9–16, 2004. Morb. Mortal. Wly. Rep. 53: 1071–1072.

Crist, E. P., and R. C. Cicone. 1984. A physically-based transformation of Thematic Mapper data – the TM Tasseled Cap. IEEE Trans. Geosci. Remote Sensing GE 22: 256–263.

Dale, P. E., and C. D. Morris. 1996. Culex annulirostris breeding sites in urban areas: using remote sensing and digital image analysis to develop a rapid predictor of potential breeding areas. J. Am. Mosq. Control Assoc. 12: 316–320.

Dale, P. E., S. A. Ritchie, B. M. Territo, C. D. Morris, A. Muhar, and B. H. Kay. 1998. An overview of remote sensing and GIS for surveillance of mosquito vector habitats and risk assessment. J. Vector. Ecol. 23: 54–61.

Denke, P. M., and E. Spackman. 1990. The mosquitoes of Wyoming. Cooperation Extension Service, Department of Plant, Soil and Insect Sciences, College of Agriculture, University of Wyoming, Laramie, WY.

[DOE] **U.S. Department of Energy. 2002.** Powder River Basin Coalbed Methane Development and Produced Water Management Study, pp. 1–3. U.S. Department of Energy. Office of Fossil Energy and National Energy Technology Laboratory Strategic Center for Natural Gas. November 2002.

Enserink, M. 2002. West Nile's surprisingly swift continental sweep. Science (Wash., DC) 297: 1988–1989.

ERDAS, Inc. 2003. ERDAS field guide, 7th ed. Leica Geosystems GIS & Mapping, LLC, Atlanta, GA.

Gao, B. 1996. NDWI - a normalized difference water index for remote sensing of vegetation liquid water from space. Remote Sensing Environ. 58: 257–266.

Goddard, L. B., A. E. Roth, W. K. Reisen, and T. W. Scott. 2002. Vector competence of California mosquitoes for West Nile virus. Emerg. Infect. Dis. 8: 1385–1391.

Hayes, R. O., E. L. Maxwell, C. J. Mitchell, and T. L. Woodzick. 1985. Detection, identification and classification of mosquito larval habitats using remote sensing scanners in earth orbiting satellites. Bull. World Health Organ. 63: 361–374.

Hay, S. I., R. W. Snow, and D. J. Rogers. 1998. From predicting mosquito habitat to malaria seasons using remotely sensed data: practice, problems and perspectives. Parasitol. Today 14: 306.

Hayes, C. G. 1989. West Nile fever, pp. 59–88. *In* T. Monath [ed.], The arboviruses: epidemiology and ecology. CRC, Boca Raton, FL.

Kauth, R. J., and G. S. Thomas. 1976. The tasseled cap–A graphic description of the spectral-temporal development of agricultural crops as seen by Landsat, pp. 41–51. *In* Proceedings, Symposium: Machine Processing of Remotely Sensed Data, 21 June–1 July, Purdue University, West Lafayette, IN.

Laird, M. 1988. The natural history of larval mosquito habitats. Academic, San Deigo, CA.

Linthicum, K. J., C. L. Bailey, F. G. Davies, and C. J. Tucker. 1987. Detection of Rift Valley fever viral activity in Kenya by satellite remote sensing imagery. Science (Wash., DC) 235: 1656–1659.

Masuoka, P. M., D. M. Claborn, R. G. Andre, J. Nigro, S. W. Gordon, T. A. Klein, and H. Kim. 2003. Use of IKONOS and Landsat for malaria control in the Republic of Korea. Remote Sensing Environ. 88: 187–194.

Morse, D. L. 2003. West Nile virus - not a passing phenomenon. N. Engl. J. Med. 348: 2173–2174.

Naugle, D. E., C. L. Aldridge, B. L. Walker, T. E. Cornish, B. J. Moynahan, M. J. Holloran, K. Brown, G. D. Johnson, E. T. Schmidtman, R. T. Mayer, et al. 2004. West Nile virus: pending crisis for greater sage-grouse. Ecol. Lett. 7: 704–713.

Nuccio, V. 2001. Geological overview of coalbed methane. U.S. Geological Survey, Open File Report 01-235.

Philipson, W. R., and W. R. Hafker. 1981. Manual versus digital analysis for delineating river flooding. Photogrammetric Engine. & Remote Sensing 47: 1351–1356.

Pope, K. O., E. J. Sheffner, K. J. Linthicum, C. L. Bailey, T. M. Logan, E. S. Kasischke, K. Birney, A. R. Njogu, and C. R. Roberts. 1992. Identification of central Kenyan Rift Valley Fever virus vector habitats with Landsat TM and evaluation of their flooding status with airborne imaging radar. Remote Sensing Environ. 40: 185–196.

Reisen, W. 1993. The western encephalitis mosquito, *Culex tarsalis.* Wing Beats 4: 16.

Rice, C. A., M. S. Ellis, and J. H. Bullock, Jr. 2000. Water co-produced with coalbedmethane in the Powder River Basin, Wyoming: preliminary compositional data. U.S. Geological Survey Open-File Report 00-372.

Rogers, D. J., M. F. Myers, C. J. Tucker, P. F. Smith, D. J. White, B. Backenson, M. Eidson, L. D. Kramer, B. Bakker, and S. I. Hay. 2002. Predicting the distribution of West Nile fever in North America using satellite sensor data. Photogrammetric Engine. & Remote Sensing 68: 112–114.

Thomson, M. C., S. J. Connor, P.J.M. Milligan, and S. P. Flasse. 1996. The ecology of malaria - as seen from Earth-observation satellites. Ann. Trop. Med. Parasitol. 90: 243–264.

U.S. Geological Survey. 2004. West Nile maps. (http://westnilemaps.usgs.gov/).

Washino, R. K., and B. L. Wood. 1994. Application of remote sensing to vector arthropod surveillance and control. Am. J. Trop. Med. Hyg. 50 (6 Suppl): 134–144.

Wood, B. L., L. R. Beck, R. K. Washino, K. Hibbard, and J. S. Salute. 1992. Estimating high mosquito-producing rice fields using spectral and spatial data. Int. J. Remote Sensing 13: 2813–2826.

[WOGCC] **Wyoming Oil and Gas Conservation Commission. 2005.** CBM data. (http://wogcc.state.wy.us).

Wyoming Outdoor Council and Powder River Basin Resource Council. 2004. Coalbed methane Development in Wyoming's Powder River Basin: Natural Gas Development and Its Threats to the Landscape, People, and Wildlife. (http://www.wyomingoutdoorcouncil.org/programs/cbm/publications.php).

Received 14 December 2005; accepted 17 February 2006.